European Journal of Control 47 (2019) 53–63

Contents lists available at ScienceDirect

European Journal of Control

journal homepage: www.elsevier.com/locate/ejcon

A Hierarchical Algorithm for Vehicle-to-Grid Integration under Line Capacity Constraints☆

Andres Cortés, Sonia Martínez*

Department of Mechanical and Aerospace Engineering, University of California, San Diego, 9500 Gilman Drive La Jolla, CA 92093-0411

ARTICLE INFO

Article history:
Received 2 July 2017
Revised 30 April 2018
Accepted 13 July 2018
Available online 19 July 2018

Recommended by Prof. G Damm

Keywords:
Electric Vehicles
Hierarchical optimization
Transactive Energy
Capacity Constraints

ABSTRACT

This work deals with the coordinated charging/discharging of a population of plug-in electric vehicles (PEVs) under energy efficiency, SOC, battery capacity, and power-line capacity constraints, to minimize energy cost. To address this, we introduce a framework in which the power grid is modeled as an undirected rooted tree, the root of this tree represents the generation/transmission side of the system and the leaves represent PEVs. Due to the several constraints, we are led to a non-convex optimization problem formulation subject to a complementarity constraint. We then show how a relaxed version of the problem can capture a wide set of optimal solutions for the original problem. After this, we propose a hierarchical algorithm for the computation of the PEVs' charging/discharging profiles based on the relaxed problem formulation. The root generates a control signal based on the price per unit of power according to the demand for each time. Intermediate nodes represent congestible elements on the distribution side (e.g., transformers), which have a bound on the demand they can satisfy. In the proposed algorithm, intermediate nodes modify the control signal according to the difference between the demand they take care of, and its capacity upper bound. PEVs update their charging/discharging strategies according to this pricing signal. A proof of algorithm convergence to the optimizer of the problem is provided. Simulations demonstrate the algorithm performance and convergence rate.

1. Introduction

As awareness toward climate change and greenhouse emissions increases, clean alternatives for energy generation and transportation are being actively investigated. Plug-in Electric vehicles (PEVs) are accepted as a promising solution to the problem of clean transportation. However, a large penetration of PEVs in an uncoordinated way may produce adverse effects on the grid operation. A possible solution is that PEVs deliver/absorb power to the grid in order to provide ancillary services [1]. To this end, PEVs' batteries can charge when there is generation excess, or to inject power if there is demand excess, e.g., peak times. In providing an algorithmic solution to this problem one can follow a centralized or decentralized approach. While centralized approaches can lead to optimized solutions in a faster manner, decentralized algorithms allow users to interact directly, in a way that does not require the exact communication of their habits, thus helping preserve privacy (e.g. by means of aggregated power usage corrupted by a differentially private mechanism) and reducing the computation burden at a central site. Motivated by this, in this manuscript, we propose a hierarchical architecture in which intermediate aggregators coordinate with PEVs an optimal Vehicle-to-Grid (V2G) charging strategy. In V2G, PEVs are able to inject energy back into the grid based on a coordination signal, keeping at sight the objective of collecting enough energy to satisfy the PEV user's requirement. To do so, intermediate pricing and aggregated load signals are employed, which helps with privacy preservation goals.

Most of the literature on PEV integration is oriented to the so-called Vehicle-one-Grid (V1G) paradigm, in which PEVs use their load flexibility to shift their own demand over time, without feeding any energy into the grid, see [2,3,4]. This allows to use the grid optimally over time, avoiding the need for capacity increases that would be required under uncoordinated charging. These works fall under the category of centralized algorithms, since all the computation is carried out by a single processor. In [5] the authors present an iterative approach to charge EVs tied to the distribution grid. The centralized algorithm checks the EV charging profile for decoupled power flow feasibility, and if the profile is not feasible, new constraints are defined at the distribution buses of the grid. This approach is also centralized, and the power flow

☆ This research was supported by the grant NSF-CMMI 1434819 and by the ARPA-e cooperative agreement DE-AR0000695.

* Corresponding author at.
E-mail addresses: andrescortes4500@gmail.com (A. Cortés), soniamd@ucsd.edu, soniamd@soe.ucsd.edu (S. Martínez).

https://doi.org/10.1016/j.ejcon.2018.07.003
0947-3580/

feasibility is studied via a decoupled power flow analysis. Other works [6,7] present a hierarchical solution to the V1G problem. In these papers, a pricing signal is transmitted by the utility to all PEVs, which update their charging strategy by solving a local optimization problem. Their updated charging strategy is then fed back to an aggregator located at the utility which computes an updated pricing signal. In [8], a similar coordination signal is used for hierarchical PEV charging control, but the charging strategy is computed using a load balancing algorithm. In [9], the authors propose an approach to reach an optimal solution to the EV charging problem in a decentralized manner. However, this approach solves local optimization problems and no comparison of the obtained solution to the optimal one is provided. This manuscript is closer to the work reported in [10], which presents various algorithms for hierarchical V1G over a grid with line capacity constraints, and batteries subject to capacity constraints. However, the algorithms in [10] require the execution of inner loop iterations, which significantly increase computational and communication cost. In [11], the authors propose the application of the Alternating Direction Method of Multipliers (ADMM) method to find a decentralized algorithm that allows a Virtual Power Plant manage a group of EVs to solve an optimal-tracking (demand response) problem. The EVs and power grid are similarly-constrained as in [10], participating in a V1G capacity, however the algorithms do not require inner loop iterations as in [10]. In [13] and [12], the authors address a coordination problem for controllable loads and PEVs respectively in a distribution network with capacity constraints. The work [14] also employs ADMM to coordinate PEVs using an aggregator. However, the problem to be solved has a completely decomposable cost function, i.e., it is the sum of local cost functions for each PEV and for an aggregator. In our work, the cost function is a sum of convex functions of the aggregated load. This couples the variables associated to each PEV in a way that ADMM cannot be directly implemented. In [15] the authors present a distributed algorithm to solve a PEV coordination problem that considers battery degradation. Their study, as well as all the aforementioned ones, does not consider the PEVs injecting power into the grid, which is a situation in which taking into account battery degradation and state of charge may play an important role in the optimization problem.

For V2G, where PEVs inject power into the grid, available works include [16], where a centralized optimization problem is solved using simulated annealing and ant-colony optimization algorithms. Further, [17] presents a purely centralized optimal control algorithm to solve a V2G problem with uncertainty. A V2G game-theoretic formulation is given in [18], where PEVs are modeled as batteries that aim to inject to or draw from an aggregator a certain amount of energy in order to meet a desired energy state in such aggregator. This study does not consider battery dynamics. Unlike this manuscript, none of the aforementioned V2G works consider any distribution grid related constraint, or grid topology model.

Here, we present a novel hierarchical V2G optimization algorithm for the coordination of a fleet of PEVs connected to different points of the distribution side of the power grid. With respect to previous work, our novel V2G problem scenario considers simultaneously SOC, capacity, and efficiency constraints for EV batteries, together with distribution line capacity constraints. Our power grid is modeled as a rooted tree graph, where the root node is the generation/transmission section of the grid, including the distribution substations. In this model, agents or nodes represent buses on the distribution feeder, and PEVs are modeled as leaves of the tree. We then exploit this hierarchy to define the communication structure of our V2G HIERARCHICAL coordination algorithm. In this approach, all PEVs solve a local optimization problem to compute their charging/discharging profile over a finite discrete-time horizon. Then, they communicate it to the bus they are connected to, this aggregates its PEV and its non-PEV load, and sends it to the next bus up in the hierarchy. The aggregation is performed in a cascaded manner until the overall load reaches the root node, which employs such information to compute a control signal that is down-streamed through the tree. As this signal passes through each bus, it is modified to account for the capacity limitations of the transmission lines that carry power to such bus. A final modified signal reaches each PEV, which employs it to recompute their charging/discharging profile. An advantage of this approach is that PEVs do not have to provide directly private information on their usage to the power-grid operator, but to the intermediate aggregators. Additionally, almost the entire computational load falls on the PEVs, while all buses in the network only act as aggregators. This results into good scalability properties of the algorithm. An important contribution of this work is the fact that our algorithm is proven to converge to the optimal solution to the proposed PEV charging/discharging problem. Additionally, with the hierarchical decision-making structure presented here and the relaxation approach for the line capacity constraints, other decomposition approaches can be adapted.

A significant contribution of our work tackles the challenge of modeling charge and discharge of batteries subject to efficiency losses while avoiding simulataneous charge and discharge. This would require either to model charge and discharge separately and impose a complementarity constraint on them, or have a single dispatch variable and a non-linear mixed-integer formulation with a switched efficiency parameter that changes when the battery dispatch changes sign. We choose the former and provide a theoretical result that allows to relax the complementarity constraint between charge and discharge under a general set of conditions. The results proves that the optimal solution still satisfies the complementarity property, even though it is not explicitly enforced for in the relaxation.

Finall, simulations show the V2G HIERARCHICAL algorithm performance on various scenarios. This work streamlines, extends and completes the preliminary work appeared in [19] in several ways. Here, we provide a proof of convergence for the main algorithm, we characterize the size of the penalization parameters needed to achieve a desired tolerance in the global constraints, and provide a more comprehensive simulation analysis of the algorithm.

1.1. Basic notation

Let $\mathbb{R}$ denote the set of real numbers, and $\mathbb{R}^n$ the n-dimensional real vector space. In what follows, $\|x\|$ represents the Euclidean norm of $x \in \mathbb{R}^n$ and $|x|$ denotes the absolute value of $x \in \mathbb{R}$. For a finite set $\mathcal{A}$, we let $|\mathcal{A}|$ denote the cardinality of $\mathcal{A}$. Given a set $\mathcal{B}$, we denote $\mathcal{A} \setminus \mathcal{B} \triangleq \{a \in \mathcal{A} \mid a \notin \mathcal{B}\}$.

2. Problem formulation

Consider a population of N plug-in electric vehicles (PEV) that are connected to the power grid. This population is spread over a large area, meaning that PEVs are connected to distinct points of the distribution grid. The objective of each PEV is to decide a charging/discharging schedule that allows them to collect the energy required by the user before a certain deadline. The capacity of PEVs to discharge power into the grid, along with the time-flexibility to charge the battery, allows users to provide a combination of energy time-shift and load deferral. This allows PEVs to provide operation benefits to the power grid.

In this section, we formulate the mathematical framework and models that are used in the sequel while introducing notation. We will consider discrete-time dynamical models, where all state and decision variables are indexed by the set of natural numbers. In this way, we divide a finite-time horizon line into T intervals of constant duration Δ. We index each of these intervals by

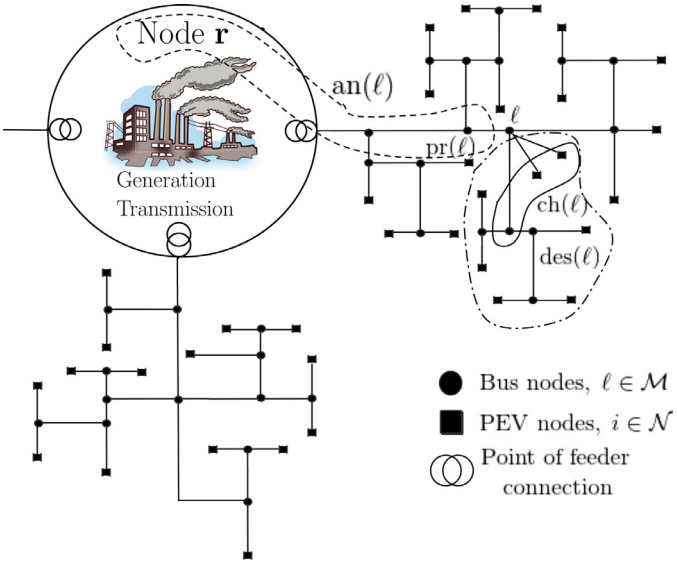

Fig. 1. Graph model of the power grid. Node **r** represents the generation/transmission part of the grid, along with the connection points of the distribution feeders. For a bus b, the set inside dashed-line boundary are its ancestors, $\mathrm{an}(b)$, the parent of b is its immediate ancestor, $\mathrm{pr}(b)$, the children of b, $\mathrm{ch}(b)$, is the set inside a continuous boundary, which is contained in the set of descendants of b, $\mathrm{des}(b)$, or the set contained within a dash-dot boundary line. The set $\mathrm{dN}(b)$ are all the PEVs that belong to $\mathrm{des}(b)$. Similar sets $\mathrm{an}(i)$, $\mathrm{pr}(i)$ can be defined for a PEV $i \in \mathcal{N}$.

$t \in \{1, \dots, T\} \subseteq \mathbb{N}$, and the charging/discharging scheduling of the PEVs is also described in terms of variables indexed by t.

2.1. Structure of the power network

The power grid is composed of three easily discernible layers: generation, transmission, and distribution. We assume that the distribution side of the grid is composed of radial feeders only (with tree topology), and each feeder has a single connection point to the transmission grid. This is a reasonable assumption, as most existing distribution feeders have this structure.

We use the rooted tree notion to model the distribution network and its interaction with the transmission/generation side of the grid, as well as with the population of PEVs. More precisely, consider an undirected graph $\mathcal{G} \triangleq (\mathcal{V}, \mathcal{E})$, where $\mathcal{V}$ is the set of nodes and $\mathcal{E}$ is the set of edges. A *path* $\mathcal{P}(i, j)$, in $\mathcal{G}$ for nodes $i, j \in \mathcal{V}$, is defined as a sequence of nodes $\{i_1, \dots, i_m\}$ such that $i_1 = i$, $i_m = j$ and (i_l, i_{l+1}) is an edge of $\mathcal{G}$, for all $\ell \in \{1, \dots, m-1\}$. A graph $\mathcal{G}$ is a tree if there is a unique path between any two nodes $i, j \in \mathcal{V}$. The distance from node i to node j in $\mathcal{G}$ is given by the number of edges in the path $\mathcal{P}(i, j)$. For an undirected tree, any $\mathbf{r} \in \mathcal{V}$ can be called a *root* of $\mathcal{G}$. In this way, the power grid is represented by an undirected rooted tree $\mathcal{T} \triangleq (\mathcal{V}, \mathcal{E})$, with the generation/transmission side of the grid be condensed in the root node **r** of the tree, see Fig. 1. All the distribution feeders that we consider in our model branch out of the root, and all the buses in these distribution feeders are represented by nodes of $\mathcal{T}$.

For a node $\ell \in \mathcal{V}$, the set of its *children*, $\mathrm{ch}(\ell)$, is composed by all the nodes that are connected by a single link to ℓ, and whose distance to **r** is larger than that of ℓ. The set of *descendants* of ℓ, $\mathrm{des}(\ell)$, is the set of all nodes $\ell' \in \mathcal{V} \setminus \{\ell\}$ such that $\ell' \in \mathcal{P}(\mathbf{r}, \ell)$. Similarly, the *parent* of ℓ, denoted as $\mathrm{pr}(\ell)$, is the unique node that is connected to ℓ by a single edge, and belongs to $\mathcal{P}(\mathbf{r}, \ell)$. The set of *ancestors* of ℓ, denoted by $\mathrm{an}(\ell)$, is the set of all nodes in $\mathcal{P}(\mathbf{r}, \ell) \setminus \{\ell\}$. A node $i \in \mathcal{V}$ is called a *leaf* of $\mathcal{G}$ if it is only connected to one node $\ell \in \mathcal{V} \setminus \{\mathbf{r}\}$. See Fig. 1 for an illustration of these concepts.

In what follows, we distinguish $\mathcal{M} \subset \mathcal{V}$ to be the set of nodes of $\mathcal{T}$ that consist of the distribution nodes and the root node. In addition, the set of PEVs attached to such buses are also nodes of $\mathcal{T}$ and included in the set $\mathcal{V}$. Without loss of generality, let us define $\mathcal{N} \triangleq \{1, \dots, N\}$, to index the set of PEVs, and $\mathcal{M} \triangleq \{N+1, \dots, \mathbf{r}\}$. Given $\ell \in \mathcal{M}$, we define the subset of its children which are also PEVs as $\mathrm{dN}(\ell) \triangleq \mathrm{des}(\ell) \cap \mathcal{N}$. In our tree model, all edges $(l_1, l_2) \in \mathcal{E}$, such that $l_1, l_2 \in \mathcal{M}$, represent distribution lines. Each distribution line (l_1, l_2), has an associated parameter $P^{\max}_{l_1 l_2}(t)$ that corresponds to an upper bound on the amount of power that can go through the line. This limitation represents the thermal limit of the distribution line. Likewise, there is a maximal amount of power $P^{\max}_{\mathbf{r}}(t)$ that the grid generation represented by node **r** can provide at each time $t \in \tau$.

2.2. PEV battery model

We assume that the battery of each PEV follows the dynamics:

$$z_{i,t} = z_{i,t-1} + \frac{\alpha^c_i}{\beta_i} u_{i,t} - \frac{1}{\alpha^d_i \beta_i} v_{i,t},$$

where $u_{i,t} \geq 0$ is the charging power for the battery during time interval $t \in \tau$, $v_{i,t} \geq 0$ is the power discharged from the battery during time $t \in \tau$, $\alpha^c_i \in (0, 1)$ is the battery system charging efficiency, $\alpha^d_i \in (0, 1)$ is the battery system discharging efficiency, β_i is a parameter that consists of the battery energy capacity divided by the duration of each time interval $t \in \tau$, and $z_{i,t}$ is the state of charge (SOC) at the end of time interval $t \in \tau$. The SOC must satisfy that $z_{i,t} \in [z_{i,\min}, z_{i,\max}]$, for $0 \leq z_{i,\min} < z_{i,\max} \leq 1$. In addition, some power bounds must be established in the battery charging/discharging, namely $u_{i,t} \leq u_{i,\max}$ and $v_{i,t} \leq v_{i,\max}$. Then, the charging/discharging action of each PEV can be characterized by a demand profile $\delta_i \triangleq (\delta_{i,1}, \dots, \delta_{i,T})$, where $\delta_{i,t} \triangleq u_{i,t} - v_{i,t}$, $i \in \mathcal{N}$ and $t \in \tau$. It is important to note that since it is not physically possible that the battery charges and discharges at the same time, $u_{i,t} v_{i,t} = 0$ must hold for all $t \in \tau$.

Linear difference equations have been used to model batteries from lead-acid to Li-Ion in several works and software tools used in academic studies as well as in industry [6,7,20,21]. The model we use in the present work is an extension of the one introduced in [6], with the difference that our model accounts for energy discharge to the grid, and the consequent efficiency losses. It captures the main power balance parameters that affect the performance of an electro-chemical storage system.

The goal for a PEV is to collect a certain amount of energy in order to be able to operate. Let $Z_i \subset \tau$, for all $i \in \mathcal{N}$ be a set of times at which the i^{th} vehicle has access to the power grid. Then, it must hold that $z_{i,q} \geq z_{i,\mathrm{op}}$, where $z_{i,\mathrm{op}}$ is the minimum SOC to be collected and $q = \max Z_i$ is the deadline for reaching that SOC.

2.3. Load buses in the distribution feeders

As it has been stated in Subsection 2.1 each of the nodes $\ell \in \mathcal{M} \setminus \mathbf{r}$ represents a bus in a distribution feeder. The bus is characterized by a demand profile $d_\ell \triangleq \{d_{\ell,t}\}_{t \in \tau}$ associated to it. This demand is the aggregate of the non-PEV demand attached to the node ℓ, denoted by $L_{\ell,t} \geq 0$, with the demand of all nodes that are children of node ℓ, i.e.:

$$d_{\ell,t} \triangleq \sum_{\ell' \in \mathrm{ch}(\ell)} d_{\ell',t} + L_{\ell,t}, \tag{1}$$

where, with a slight abuse of notation, we identify $d_{i,t} \equiv \delta_{i,t}$, for $i \in \mathcal{N}$. Notice that $\mathrm{ch}(\ell)$ can either be PEVs or other nodes in $\mathcal{M} \setminus \mathbf{r}$, thus the expression in (1) is a recursion that can be written

in terms of the descendants of ℓ as follows:

$$d_{\ell,t} \triangleq L_{\ell,t} + \sum_{\ell' \in \mathrm{des}(\ell)\cap\mathcal{M}} L_{\ell',t} + \sum_{\ell' \in \mathrm{dN}(\ell)} \delta_{\ell',t}, \tag{2}$$

\vskip-\lastskip\pagebreak for all $\ell \in \mathcal{M} \setminus \mathbf{r}$, where recall that $\mathrm{dN}(\ell) \triangleq \mathcal{N} \cap \mathrm{des}(\ell)$. Since PEVs may be descendants of node ℓ, $d_{\ell,t}$ may be negative, which means that power is flowing upstream from node ℓ toward its parent $\mathrm{pr}(\ell)$.

Remark 2.1. Notice that the power flowing through line (ℓ, ℓ'), $\ell, \ell' \in \mathcal{M}$ at time $t \in \tau$ is given by $d_{\ell,t}$, if $\ell' \in \mathrm{pr}(\ell)$, and $d_{\ell',t}$ if $\ell \in \mathrm{pr}(\ell')$. This comes from the radial structure of all distribution feeders and the fact that the demands $d_{\ell,t}$ and $\delta_{i,t}$ must be satisfied for all $\ell \in \mathcal{M}$ and $i \in \mathcal{N}$, and for all $t \in \tau$. Given the rooted tree structure of the network, there is a one-to-one correspondence between nodes in $\mathcal{M} \setminus \{\mathbf{r}\}$ and the transmission lines in the distribution side. Then, in order to account for the bounds in the transmission capacity, for all distribution lines, it suffices to pose the following constraints:

$$|d_{\ell,t}| \le P^{\max}_{\ell\mathrm{pr}(\ell)}(t), \quad \forall t \in \tau, \ell \in \mathcal{M} \setminus \{\mathbf{r}\},$$

where, consistent with the notation, $P^{\max}_{\ell\mathrm{pr}(\ell)}(t)$ is the transmission capacity of the line between j and its parent. Therefore, for simplicity of notation, we denote the capacity of the line between j and its parent by $P^{\max}_{\ell}(t)$, leading to:

$$|d_{\ell,t}| \le P^{\max}_{\ell}(t), \quad \forall t \in \tau, \ell \in \mathcal{M} \setminus \{\mathbf{r}\}.$$

Unlike static storage systems, PEVs still behave more often like loads rather than generators, since their primary objective is to replenish the battery in order to satisfy the owner's usage objective. Therefore, it is expected from PEVs to inject power into the grid only when system load peaks are high enough or when a thermal limit constraint in the distribution circuit is susceptible to be violated due to excess load. Since the peak shaving operation aims to only reduce the peak, it is not expected that the PEVs will generate a large enough reverse flow to activate thermal constraints, so in general it will be the case that $d_{\ell,t} > -P^{\max}_{\ell}(t)$, for $\ell \in \mathcal{M} \setminus \{\mathbf{r}\}$.

2.4. The generation/pricing node

The node $\mathbf{r} \in \mathcal{V}$, referred to as the generation/price node models the behavior of the generation/transmission side of the power grid. For simplicity, we consider that this node has the a finite capacity to provide power to the distribution feeders connected to it. It is worth noticing that the demand profile $d_{\mathbf{r},t}$, $t \in \tau$, represents the aggregate demand of the entire distribution grid at time, given by:

$$d_{\mathbf{r},t} \triangleq \sum_{\ell \in \mathrm{ch}(\mathbf{r})} d_{\ell,t}.$$

Therefore, the node $\mathbf{r}$ is represented by its demand profile, the maximum amount of power that it can provide, denoted by $P^{\max}_{\mathbf{r}}(t)$, and the generation cost for the energy supplied by the grid at time $t \in \tau$. This generation cost is given by $C : \mathbb{R} \to \mathbb{R}$, which is a convex and increasing function of its argument. The argument of this function corresponds to the aggregate power that is provided by the grid to the loads at time t. The function C models an electricity price that increases as the demand increases and decreases if demand decreases. Since this function is intended to shape user behavior, C is designed to a great extent by the grid operator. It is envisioned that the PEVs and users are actually managed by intermediate aggregators which act on their behalf to interact with the larger power grid operator. We make the following assumption:

Assumption 2.1 (Derivative of C is Lipschitz). The function C is such that C' is Lipschitz in its domain, with Lipschitz constant l_C.

2.5. Optimal control problem

The charging strategy is devoted to minimize a function corresponding to the total cost of the energy provided by the utility during a finite horizon T, subject to user needs and line capacity constraints. Taking into account the consideration in Remark 2.1, we formulate the following optimization problem:

Problem 1: $\min_{u,v} J(u, v)$

subject to:

$$(u_i, v_i) \in \mathcal{F}_i, \quad \forall i \in \mathcal{N}, \tag{3a}$$

$$\delta_{i,t} = u_{i,t} - v_{i,t}, \quad \forall t, i \in \mathcal{N}, \tag{3b}$$

$$d_{\ell,t} = \textstyle\sum_{\ell' \in \mathrm{ch}(\ell)} d_{\ell',t} + L_{\ell,t}, \quad \forall t, \ell \in \mathcal{M}, \tag{3c}$$

$$|d_{\ell,t}| \le P^{\max}_{\ell}(t), \quad \forall t, \ell \in \mathcal{M} \setminus \{\mathbf{r}\}, \tag{3d}$$

$$|d_{\mathbf{r},t}| \le P^{\max}_{\mathbf{r}}(t), \quad \forall t. \tag{3e}$$

Here,

$$J(u, v) = \sum_{t=1}^{T} C(d_{\mathbf{r},t}). \tag{4}$$

and the set $\mathcal{F}_i$ is defined as

$$\mathcal{F}_i = \{(u, v) \in \mathbb{R}^{2nT} | (5a) \text{ through } (5h) \text{ hold } \forall\, i \in \mathcal{N}, \quad t \in \tau\},$$

where

$$z_{i,t} = z_{i,0} + \tfrac{1}{\beta_i} \textstyle\sum_{\ell=1}^{t} \left(\alpha_i^c u_{i,\ell} - \tfrac{1}{\alpha_i^d} v_{i,\ell}\right), \quad t \in \tau, \tag{5a}$$

$$z_{i,\min} \le z_{i,t} \le z_{i,\max}, \quad t \in \tau, \tag{5b}$$

$$0 \le u_{i,t} \le u_{i,\max}, \quad t \in \tau, \tag{5c}$$

$$0 \le v_{i,t} \le v_{i,\max}, \quad t \in \tau, \tag{5d}$$

$$u_{i,t} = 0, \quad t \notin Z_i \subseteq \tau, \tag{5e}$$

$$v_{i,t} = 0, \quad t \notin Z_i \subseteq \tau, \tag{5f}$$

$$z_{i,T} \ge z_{i,\mathrm{op}}, \tag{5g}$$

$$u_{i,t} v_{i,t} = 0, \quad t \in \tau. \tag{5h}$$

Remark 2.2. The usage objective can be more complicated than a deadline. Our present approach can integrate the usage model presented in [8] which accounts for departure times and travel requirements. However, for the sake of clarity in our analysis, we do not include it this manuscript.

Notice that constraint (5g) is a reformulation of the deadline constraint, using the fact that $z_{i,T} = z_{i,q}$ for $q = \max Z_i$. Also notice that (5h) makes the problem non-convex. In what follows, we will relax this non-convex constraint. We conjecture that the solutions of the relaxed optimization problem will satisfy this constraint in most of the cases, which depends on the problem parameters. The following result provides a characterization of such solutions, which are in the interior of the feasible set by an amount depending on $1 - \max_{i\in\mathcal{N}} \alpha_i^c \alpha_i^d$ or for a relaxed version of Problem 1 in which the lower bounds on $d_{\ell,t}$, $\ell \in \mathcal{M}$, $t \in \tau$, are dropped.

Lemma 2.1 (On the relaxation of Problem 1). *The optimal solutions for the relaxed version of Problem 1, (u, v) which satisfy the constraints (5b) and (5g) with strict inequalities, and are*

such that (3d) and (3e) hold as $-P_\ell^{\max}(t)+\epsilon < d_{\ell,t} < P_\ell^{\max}(t)$ *for* $\epsilon \geq \max_{i\in\mathcal{N}}\{(1-\alpha_i^c\alpha_i^d)u_{\max}, ((\alpha_i^c\alpha_i^d)^{-1}-1)v_{\max}\}$, *must also satisfy (5h). In addition, if the constraint (3d) and (3e) are replaced by* $d_{\ell,t} \leq P_\ell^{\max}(t)$ *for all* t *and* $j \in \mathcal{M}$, *then the relaxation of the problem becomes exact for any choice of parameters.*

The proof of the lemma can be found in Appendix A. In what follows, we assume that the solutions of Problem 1 satisfy the assumptions of the lemma.

The next result is an adaptation of Theorem 1 in [7], and shows the uniqueness of the optimal demand profile generated by the optimizers of Problem 1.

Lemma 2.2 (Uniqueness of the aggregate demand profile). *Let* $u^\star, v^\star$ *and* $\hat{u}, \hat{v}$ *be optimizers of Problem 1. Then it holds that* $\sum_{i\in\mathcal{N}}(u_i^\star - v_i^\star) = \sum_{i\in\mathcal{N}}(\hat{u}_i - \hat{v}_i)$.

The solution of this optimization problem is *valley filling* and *peak-shaving*, i.e., if u, v is optimal, the PEVs will try to provide as much energy as possible in the highest-price times and will try to obtain as much energy as possible in the lowest-price times.

In order to solve the relaxed version of Problem 1, we use penalty functions to handle the coupling constraints. We formulate the following relaxation of the problem:

$$\text{Problem 2:}\quad \min_{u,v} J(u,v) + \sum_{t=1}^{T}\sum_{\ell\in\mathcal{M}} \kappa_\ell \Phi_\ell(d_{\ell,t})$$

subject to:

$$(u_i, v_i) \in \bar{\mathcal{F}}_i, \quad \forall i \in \mathcal{N}, \tag{6a}$$

$$\delta_{i,t} = u_{i,t} - v_{i,t}, \quad \forall t, i \in \mathcal{N}, \tag{6b}$$

$$d_{\ell,t} = \sum_{\ell'\in \mathrm{ch}(\ell)} (d_{\ell',t} + L_{\ell,t}), \quad \forall t, \ell \in \mathcal{M}, \tag{6c}$$

where $\Phi_\ell : \mathbb{R} \to \mathbb{R}_{\geq 0}$ acts as a penalty function for the power constraint at node $\ell \in \mathcal{M}$, defined as:

$$\Phi_\ell(d_{\ell,t}) \triangleq \max\{0, d_{\ell,t} - P_\ell^{\max}(t)\}^2,$$

$\kappa_\ell > 0$, for $\ell \in \mathcal{M}$, and

$$\bar{\mathcal{F}}_i = \{(u,v) \in \mathbb{R}^{2nT} \,|\, (5a) \text{ through } (5g) \text{ hold } \forall i \in \mathcal{N}, t \in \tau\}.$$

Notice that:

$$\Phi'_\ell(d_{\ell,t}) = \max\{0, 2(d_{\ell,t} - P_\ell^{\max}(t))\},$$

then, $\Phi'_\ell(d_{\ell,t})$ is globally Lipschitz continuous with Lipschitz constant $l_B = 2$, for all $\ell \in \mathcal{M}$.

2.6. Analysis and design of the penalty method

From [22], it is known that for the penalty method to yield a feasible solution to the original problem, it is necessary to use non-differentiable penalty functions, except for selected cases, which our problem does not satisfy. Clearly, the quadratic penalty functions are continuously differentiable, therefore the solution to Problem 2 may not be feasible for Problem 1. However, it is also known that if $\kappa_\ell \to +\infty$, for all $\ell \in \mathcal{M}$, the solution to Problem 2 will get arbitrarily close to a solution to Problem 1.

Lemma 2.3. *If an optimal solution to Problem 2 satisfies the constraints (3d) (3e) and (5h), then such solution is also an optimal solution of Problem 1.*

By the result above, we have that a solution to Problem 2 is not a solution to the relaxed version of Problem 1 only if it violates at least one of the constraints given by (3d) or (3e). Therefore, a suitable way to study how close the solution to Problem 2 is to a solution to Problem 1, is to analyze the maximum amount of constraint violation for a given value of the parameters κ_ℓ, for all $\ell \in \mathcal{M}$. In this way, one can design parameters κ_ℓ that lead to a desired tolerance on the constraint violation. To this end, we introduce the following assumption.

Assumption 2.2 (Slater's Condition). There exists a feasible solution $u^\dagger, v^\dagger$ to the relaxed version of Problem 1, such that:

$$d^\dagger_{\ell,t} \leq P_\ell^{\max}(t) - \varepsilon, \quad \ell \in \mathcal{M},$$

for all $t \in \tau$, such that $P_\ell^{\max}(t) - \varepsilon > 0$, $\varepsilon > 0$ and does not depend on ℓ.

The following result establishes how to choose all parameters κ_ℓ.

Proposition 2.1 (Characterization of κ_ℓ). *Fix* $\sigma \in (0,1)$ *and let* $\kappa_\ell > \sqrt{|\mathcal{M}|T}(J_{\max} - J_{\min})/(\varepsilon\sigma \min_{\ell,t} P_\ell^{\max}(t))$, *for all* $\ell \in \mathcal{M}$, *where*

$$J_{\max} \triangleq \sum_{t=1}^{T} C(P_{\mathbf{r}}^{\max}(t)), \qquad J_{\min} \triangleq \sum_{t=1}^{T} C(-P_{\mathbf{r}}^{\max}(t))$$

Let $u^\star, v^\star$ *be a solution to Problem 2. Then,* $u^\star, v^\star$ *satisfies:*

$$d^\star_{\ell,t} \leq P_\ell^{\max}(t)(1+\sigma),$$

for all $\ell \in \mathcal{M}$.

The proof of this result can be found in Appendix A.1.

3. A hierarchical control architecture

Our main interest in the present work is to solve Problem 1 using a decentralized/hierarchical communication and control architecture that allows for distributed computation, scalability, and privacy. Next, we introduce a hierarchical approach for the solution of Problem 2. For now on, let us assume that the optimization problem is feasible.

3.1. V2G hierarchical algorithm

Our approach endows each element in the grid subject to capacity limits with computation and communication capabilities. The nodes act as intermediate aggregators which communicate over the network following the tree power-grid topology. In the algorithm, each element $\ell \in \mathcal{V}\setminus\{\mathbf{r}\}$ sends its parent the aggregated demand profile d_ℓ and, if $\mathrm{ch}(\ell)\neq\emptyset$, sends its children a control signal based on information provided by generation/pricing node $\mathbf{r}$, and the amount of violation on the maximum power constraints of ℓ's ancestors.

The V2G HIERARCHICAL algorithm is inspired by the works presented in both [6,7] but we modify the approach to account for the penalty functions of Problem 2. We do not consider more standard algorithms for distributed optimization such as ADMM [23,24] or the primal-dual subgradient algorithm in [25] given the lack of flexibility they present to handle coupling constraints such the line capacity constraints in our formulation.

More precisely, at each iteration $k \in \mathbb{N}$, PEV $i \in \mathcal{N}$ generates a demand profile $\delta^k_{i,t} = u^k_{i,t} - v^k_{i,t}$, for all $t \in \tau$, which is feasible for its own battery constraints. Then, it transmits the profile to its parent, which in turn aggregates its own demand profile according to (1). This is done from the bottom up until the root node $\mathbf{r}$ computes its demand profile; see Fig. 2 for an illustration of the information flow over the communication network.

Based on its demand profile, $\mathbf{r}$ then provides a coordination signal $p^k_{\mathbf{r}} \triangleq [p^k_{\mathbf{r},1} \ldots, p^k_{\mathbf{r},T}]^\top \in \mathbb{R}^T$, such that:

$$p^k_{\mathbf{r},t} \triangleq \eta C'(d^k_{\mathbf{r},t}) + b^k_{\mathbf{r},t},$$

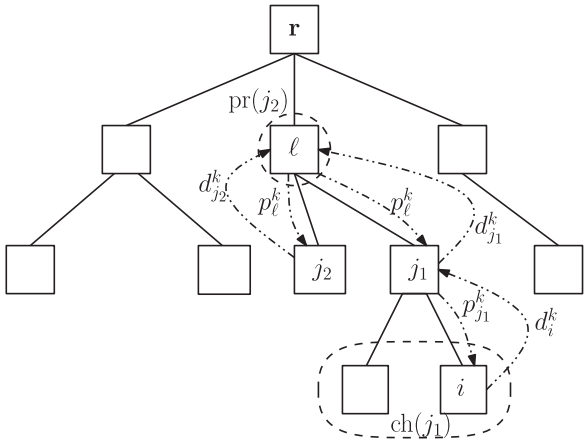

Fig. 2. Grid hierarchical structure. Dashed lines indicate communication links while solid lines represent power links.

for all $t\in\tau$, for some $\eta>0$, $b^k_{\mathbf{r},t}=\eta\kappa_{\mathbf{r}}\Phi'_{\mathbf{r}}(d^k_{\mathbf{r},t})$, with $\Phi_{\mathbf{r}}$ as introduced in Problem 2, and $\kappa_{\mathbf{r}}>0$. Then, each node $\ell\in\mathcal{M}\setminus\{\mathbf{r}\}$ computes the control signal $p^k_\ell\triangleq[p^k_{\ell,1}\dots,p^k_{\ell,T}]^\top\in\mathbb{R}^T$:

$$p^k_{\ell,t}\triangleq p^k_{\mathrm{pr}(\ell),t}+b^k_{\ell,t},$$

for all $t\in\tau$, where:

$$b^k_{\ell,t}=\eta\kappa_\ell\Phi'_\ell(d^k_{\ell,t}),$$

where Φ_ℓ is introduced in Problem 2 and $\kappa_\ell>0$. When this signal reaches each PEV i, this computes its next battery control by solving the following optimization problem:

$$\begin{aligned}(u_i^{k+1},v_i^{k+1})=\ &\mathrm{argmin}_{u_i,v_i}J_i(u_i,v_i,\delta_i^k)\\ &\text{subject to:}\\ &(u_i,v_i)\in\bar{\mathcal{F}}_i,\end{aligned}\tag{7}$$

where:

$$J_i(u_i,v_i)=\sum_{t=1}^{T}p^k_{\mathrm{pr(i)},t}(u_{i,t}-v_{i,t})+\frac{1}{2}\|u_i-v_i-\delta_i^k\|^2,\tag{8}$$

and $p^k_{\mathrm{pr(i)},t}=p^k_{\mathbf{r},t}+\sum_{\ell\in\mathrm{an}(i)\setminus\{\mathbf{r}\}}b^k_{\ell,t}$. The procedure must be iterated until a stopping criterion is met. The parameters κ_ℓ can be chosen according to Lemma 2.1 after determining the feasibility of Problem 2 and deciding upon σ. A choice of η that guarantees algorithm convergence is given next.

Theorem 3.1 (Convergence result). *The* V2G HIERARCHICAL *algorithm converges to an optimizer of Problem 2 as $k\to\infty$, provided Assumption 2.1 (on the derivative of C) holds and $\eta<\min\{\eta_1,\eta_2\}$, where:*

$$\eta_1\triangleq\min_{i\in\mathcal{N}}(Nl_C(1+|\mathrm{an}(i)|))^{-1},$$

$$\eta_2\triangleq\min_{i\in\mathcal{N},\ell\in\mathrm{an}(i)}(2\kappa_\ell|\mathrm{dN}(\ell)|(1+|\mathrm{an}(i)|))^{-1}.$$

Proof. Consider the Lyapunov function:

$$V(u,v)=\sum_{t=1}^{T}\left(C(d_{\mathbf{r},t})+\sum_{\ell\in\mathcal{M}}\kappa_\ell\Phi(d_{\ell,t})\right).$$

We show next that $V(u^{k+1},v^{k+1})\le V(u^k,v^k)$, for all $k\in\mathbb{N}$ and $V(u^{k+1},v^{k+1})=V(u^k,v^k)$ only if (u^k,v^k) is a fixed point of the algorithm. Finally, we show that a fixed point of the algorithm must be an optimizer of Problem 2.

From the convexity of C, it follows that:

$$C\big(d^k_{\mathbf{r},t}\big)-C\big(d^{k+1}_{\mathbf{r},t}\big)\ge C'\big(d^{k+1}_{\mathbf{r},t}\big)\big(d^k_{\mathbf{r},t}-d^{k+1}_{\mathbf{r},t}\big),$$

or, equivalently,

$$C\big(d^{k+1}_{\mathbf{r},t}\big)\le C\big(d^k_{\mathbf{r},t}\big)+C'\big(d^{k+1}_{\mathbf{r},t}\big)\big(d^{k+1}_{\mathbf{r},t}-d^k_{\mathbf{r},t}\big).$$

Similarly, we have that:

$$\Phi_\ell\big(d^{k+1}_{\ell,t}\big)\le\Phi_\ell\big(d^k_{\ell,t}\big)+\Phi'_\ell\big(d^{k+1}_{\ell,t}\big)\big(d^{k+1}_{\ell,t}-d^k_{\ell,t}\big),$$

for all $\ell\in\mathcal{M}$. Then, we have that:

$$\begin{aligned}V(u^{k+1},v^{k+1})\le&\sum_{t=1}^{T}\Big(C\big(d^k_{\mathbf{r},t}\big)+C'\big(d^{k+1}_{\mathbf{r},t}\big)\big(d^{k+1}_{\mathbf{r},t}-d^k_{\mathbf{r},t}\big)\Big)\\&+\sum_{t=1}^{T}\sum_{\ell\in\mathcal{M}}\kappa_\ell\Big(\Phi_\ell\big(d^k_{\ell,t}\big)+\Phi'_\ell\big(d^{k+1}_{\ell,t}\big)\big(d^{k+1}_{\ell,t}-d^k_{\ell,t}\big)\Big).\end{aligned}\tag{9}$$

Using the fact that C' is Lipschitz continuous:

$$\begin{aligned}C'\big(d^{k+1}_{\mathbf{r},t}\big)\big(d^{k+1}_{\mathbf{r},t}-d^k_{\mathbf{r},t}\big)\le&\ C'\big(d^k_{\mathbf{r},t}\big)\big(d^{k+1}_{\mathbf{r},t}-d^k_{\mathbf{r},t}\big)\\&+l_C\big|d^{k+1}_{\mathbf{r},t}-d^k_{\mathbf{r},t}\big|^2,\end{aligned}\tag{10}$$

Likewise, since Φ' is also Lipschitz continuous with Lipschitz constant equal to 2:

$$\begin{aligned}\kappa_\ell\Phi'_\ell\big(d^{k+1}_{\ell,t}\big)\big(d^{k+1}_{\ell,t}-d^k_{\ell,t}\big)\le&\ \frac{1}{\eta}b^k_{\ell,t}\big(d^{k+1}_{\ell,t}-d^k_{\ell,t}\big)\\&+2\big|d^{k+1}_{\ell,t}-d^k_{\ell,t}\big|^2.\end{aligned}\tag{11}$$

In the last expression, we have replaced $\kappa_\ell\Phi'(d^k_{\ell,t})$ by an equivalent expression based on the definition of $b^k_{\ell,t}$, $\ell\in\mathcal{M}$. Using (2) and the fact $L_{\ell,t}$ does not depend on k, for all $\ell\in\mathcal{M}$, we obtain:

$$d^{k+1}_{\ell,t}-d^k_{\ell,t}=\sum_{i\in\mathrm{dN}(\ell)}\big(u^{k+1}_{i,t}-v^{k+1}_{i,t}-u^k_{i,t}+v^k_{i,t}\big).\tag{12}$$

for all $\ell\in\mathcal{M}$. Employing now (10) and (11) to upper bound (9), and then plugging (12) into the result, we obtain:

$$\begin{aligned}V(u^{k+1},v^{k+1})\le V(u^k,v^k)&+\sum_{t=1}^{T}l_C\left|\sum_{i\in\mathcal{N}}\big(u^{k+1}_{i,t}-v^{k+1}_{i,t}-u^k_{i,t}+v^k_{i,t}\big)\right|^2\\&+\sum_{t=1}^{T}\sum_{i\in\mathcal{N}}\frac{1}{\eta}p^k_{\mathbf{r},t}\big(u^{k+1}_{i,t}-v^{k+1}_{i,t}-u^k_{i,t}+v^k_{i,t}\big)\\&+\sum_{t=1}^{T}\sum_{\ell\in\mathcal{M}\setminus\{\mathbf{r}\}}\sum_{i\in\mathrm{dN}(\ell)}\frac{1}{\eta}b^k_{\ell,t}\big(u^{k+1}_{i,t}-v^{k+1}_{i,t}-u^k_{i,t}+v^k_{i,t}\big)\\&+2\sum_{t=1}^{T}\sum_{\ell\in\mathcal{M}}\kappa_\ell\left|\sum_{i\in\mathrm{dN}(\ell)}\big(u^{k+1}_{i,t}-v^{k+1}_{i,t}-u^k_{i,t}+v^k_{i,t}\big)\right|^2.\end{aligned}\tag{13}$$

In (13), we have rewritten $C'(d_{\mathbf{r},t})+\kappa_{\mathbf{r}}\Phi'(d_{\mathbf{r},t})$ as $\frac{1}{\eta}p^k_{\mathbf{r},t}$, for all $t\in\{1,\dots,T\}$.

Further, (u_i^{k+1},v_i^{k+1}), as the solution of the local PEV problem, fulfills the condition of Appendix B for the local PEV problem. Then, we obtain:

$$\begin{aligned}\sum_{t=1}^{T}\left(p^k_{\mathbf{r},t}+\sum_{\ell\in\mathrm{an}(i)\setminus\{\mathbf{r}\}}b^k_{\ell,t}\right)\big(u^k_{i,t}-v^k_{i,t}-u^{k+1}_{i,t}+v^{k+1}_{i,t}\big)\\-\|u_i^{k+1}-v_i^{k+1}-u_i^k+v_i^k\|^2\ge0,\end{aligned}\tag{14}$$

where we have replaced the term $p^k_{\mathrm{pr(i)},t}$ by its definition, and we are using that $\sum_{t=1}^{T}|z_t|^2=\|z\|^2$, for the vectors $z=u_i-v_i\in\mathbb{R}^T$. Now, summing both sides of (14) over all $i\in\mathcal{N}$ and using Lemma B.1 in Appendix B.1 to change the summation indices, we

obtain:

$$\sum_{t=1}^{T}\sum_{i\in\mathcal{N}} p^k_{\mathbf{r},t}\left(u^{k+1}_{i,t}-v^{k+1}_{i,t}-u^k_{i,t}+v^k_{i,t}\right)$$
$$+\sum_{t=1}^{T}\sum_{\ell\in\mathcal{M}\setminus\{\mathbf{r}\}}\sum_{i\in\mathrm{dN}(\ell)} b^k_{\ell,t}\left(u^{k+1}_{i,t}-v^{k+1}_{i,t}-u^k_{i,t}+v^k_{i,t}\right)$$
$$\leq -\sum_{i\in\mathcal{N}}\|u^{k+1}_i-v^{k+1}_i-u^k_i+v^k_i\|^2. \tag{15}$$

On the other hand, from Hölder's inequality $(\sum_i(a_ib_i)\leq(\sum_i a_i^2)^{1/2}(\sum_i b_i^2)^{1/2})$ we have that:

$$\left|\sum_{i\in\mathcal{I}}\left(u^{k+1}_{i,t}-v^{k+1}_{i,t}-u^k_{i,t}+v^k_{i,t}\right)\right|^2$$
$$\leq|\mathcal{I}|\sum_{i\in\mathcal{I}}\left|u^{k+1}_{i,t}-v^{k+1}_{i,t}-u^k_{i,t}+v^k_{i,t}\right|^2, \tag{16}$$

for any subset of $\mathcal{I}\subset\mathcal{V}$. Our next step is to use (16) to bound the second and last summands of (13), with $\mathcal{I}=\mathcal{N}$ and $\mathcal{I}=\mathrm{dN}(\ell)$ respectively, then use the bound from (15) on the third and fourth summands of (13), and finally apply Lemma B.1 of Appendix D on the last summand of (13). We also use the notation $\sum_{t=1}^T|z_t|^2=\|z\|^2$, for the vectors $z=u_i-v_i\in\mathbb{R}^T$. In this way:

$$\begin{aligned}V(u^{k+1},v^{k+1})\leq{}& V(u^k,v^k)\\&+\sum_{i\in\mathcal{N}} l_C N\|u^{k+1}_i-v^{k+1}_i-u^k_i+v^k_i\|^2\\&-\sum_{i\in\mathcal{N}}\frac{1}{\eta}\|u^{k+1}_i-v^{k+1}_i-u^k_i-v^k_i\|^2\\&+\sum_{i\in\mathcal{N}}\sum_{\ell\in\mathrm{an}(i)}2\kappa_\ell|\mathrm{dN}(\ell)|\|u^{k+1}_i-v^{k+1}_i\\&-u^k_i+v^k_i\|^2.\end{aligned} \tag{17}$$

Now, it is easy to see that:

$$\frac{1}{\eta}\|u^{k+1}_i-v^{k+1}_i-u^k_i-v^k_i\|^2$$
$$=\frac{1}{\eta(1+|\mathrm{an}(i)|)}\|u^{k+1}_i-v^{k+1}_i-u^k_i-v^k_i\|^2$$
$$+\sum_{\ell\in\mathrm{an}(i)}\frac{1}{\eta(1+|\mathrm{an}(i)|)}\|u^{k+1}_i-v^{k+1}_i-u^k_i-v^k_i\|^2,$$

for all $i\in\mathcal{N}$. This follows from the fact that the term inside the sum does not depend on the index of such sum. Then, replacing the expression above in (17), it follows:

$$\begin{aligned}&V(u^{k+1},v^{k+1})\\&\leq V(u^k,v^k)+\sum_{i\in\mathcal{N}}\left(Nl_C-\frac{1}{\eta(1+|\mathrm{an}(i)|)}\right)\|u^{k+1}_i-v^{k+1}_i-u^k_i+v^k_i\|^2\\&+\sum_{i\in\mathcal{N}}\sum_{\ell\in\mathrm{an}(i)}\left(2\kappa_\ell|\mathrm{dN}(\ell)|-\frac{1}{\eta(1+|\mathrm{an}(i)|)}\right)\times\cdots\\&\|u^{k+1}_i-v^{k+1}_i-u^k_i+v^k_i\|^2.\end{aligned} \tag{18}$$

This means that $V(u^{k+1},v^{k+1})\leq V(u^k,v^k)$, if:

$$\frac{1}{\eta(1+|\mathrm{an}(i)|)}>2\kappa_\ell|\mathrm{dN}(\ell)|,\quad\forall\ell\in\mathrm{an}(i),i\in\mathcal{N}$$
$$\frac{1}{\eta(1+|\mathrm{an}(i)|)}>Nl_C,\quad\forall i\in\mathcal{N}.$$

In fact, $V(u^{k+1},v^{k+1})<V(u^k,v^k)$ whenever $u^{k+1}_i-v^{k+1}_i\neq u^k_i-v^k_i$, then the V2G HIERARCHICAL algorithm converges to the set of points $\mathcal{S}\triangleq\{(u,v)\in\mathbb{R}^{2nT}\mid\bar{u}_i-\bar{v}_i=u_i-v_i,$ and $\bar{u},\bar{v}$ are obtained from (7), for $\delta_i=u_i-v_i,\forall i\in\mathcal{N}\}$. Finally, let an equilibrium point of the algorithm be denoted as $u^\star,v^\star$. If we use the optimality condition in Appendix B for the local problem in (7), we have that

$$\sum_{t=1}^{T}p^\star_{\mathrm{pr(i)},t}(u_{i,t}-u^\star_{i,t}-v_{i,t}+v^\star_{i,t})\geq 0,\quad\forall u,v\in\overline{\mathcal{F}}_i.$$

Then, if we sum the previous set of inequalities over all $i\in\mathcal{N}$ and replace the expression for $p^\star_{\mathrm{pr(i)},t}=p^\star_{\mathbf{r},t}+\sum_{\ell\in\mathrm{an}(i)\setminus\{\mathbf{r}\}}b^\star_{\ell,t}=\eta C'(d^\star_{\mathbf{r},t})+\sum_{\ell\in\mathrm{an}(i)}\eta k_\ell\Phi'_\ell(d^\star_{\ell,t})$ into it, we obtain

$$\begin{aligned}&\sum_{t=1}^{T}\sum_{i\in\mathcal{N}}p^\star_{\mathrm{pr(i)},t}(u_{i,t}-u^\star_{i,t}-v_{i,t}+v^\star_{i,t})\\&=\sum_{t=1}^{T}(C'(d^\star_{\mathbf{r},t})+\kappa_{\mathbf{r}}\Phi_{\mathbf{r}}(d^\star_{\mathbf{r},t}))\left(\sum_{i\in\mathcal{N}}(\delta_{i,t}-\delta^\star_{i,t})\right)\\&+\sum_{t=1}^{T}\sum_{i\in\mathcal{N}}\sum_{\ell\in\mathrm{an}(i)\setminus\{r\}}\kappa_\ell\Phi'_\ell(d^\star_{\ell,t})(\delta_i-\delta^\star_i)\geq 0,\quad\forall u_i,v_i\in\bar{\mathcal{F}}_i.\end{aligned}$$

By using Lemma B.1 in Appendix D, one recovers the optimality condition for Problem 2. This implies that any point in $\mathcal{S}$ is an optimizer of Problem 2, completing the proof. □

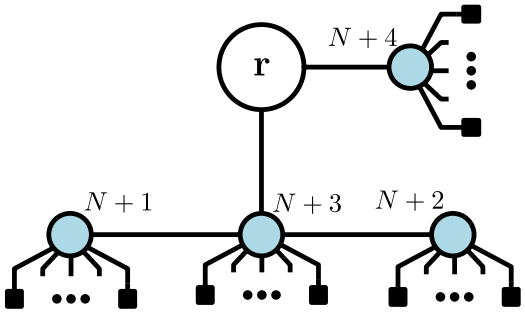

Fig. 3. Topology for the simulation scenario. Black circles denote buses in distribution feeders, while squares denote PEVs.

4. Simulations and discussion

Our simulation scenario consists in the rooted tree shown in Fig. 3, where the squares represent the PEVs and the circles represent the nodes in $\mathcal{M}$, with $\mathcal{V}=\{1,\dots,25\}$, $\mathcal{N}=\{1,\dots,20\}$, $\mathrm{pr}(i)=21$, for $i\in\{1,\dots,5\}$, $\mathrm{pr}(i)=22$, for $i\in\{6,\dots,10\}$, $\mathrm{pr}(i)=23$, for $i\in\{11,\dots,15\}$, and $\mathrm{pr}(i)=24$, for $i\in\{16,\dots,20\}$. The initial conditions, efficiency and battery capacities have been chosen to be different for all the PEVs. We establish bounds for the power to go through lines $N+1$ to $N+3$ and $N+2$ to $N+3$ as: $P^{\max}_{N+1}(t)=8.5$ and $P^{\max}_{N+2}(t)=14.5$, respectively, for all $t\in\tau$. There is no bound for other lines in the distribution feeders. The function C is chosen to be $C(x)=x^2$. All non-PEV demand, as well as the initial conditions, efficiency and battery capacities can be found at http://nodes.ucsd.edu/sonia or is available upon request.

Fig. 4 shows the optimal aggregate demand for all the PEVs in $\mathcal{N}$, for a centralized solution of the exact problem, i.e., without penalty functions (red curve), and the aggregate demand given by the V2G HIERARCHICAL algorithm after 3000 iterations (black curve). The centralized solution to Problem 1 is computed using the package `cvx`. It can be observed that the hierarchical solution almost matches the aggregate given by the centralized benchmark. Fig. 5 show the aggregate PEV and non-PEV demand for the centralized solution (red) and for the hierarchical solution (black). In addition, we show in blue the non-PEV demand. It can be seen that the optimal solution is peak-shaving and valley-filling, since PEVs tend to provide energy between 12:00 and 17:00, and they charge between 22:00 and 8:00.

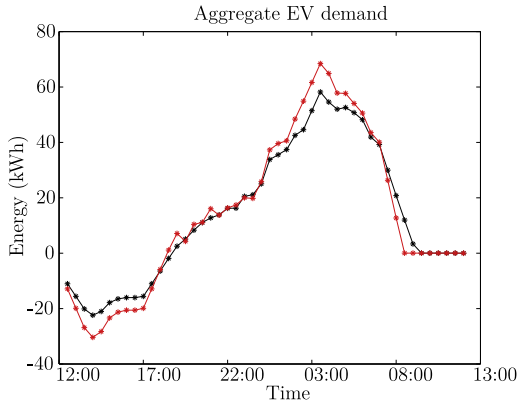

Fig. 4. The optimal aggregate EV demand is shown in red. The aggregate EV demand from the V2G HIERARCHICAL algorithm is shown in black.

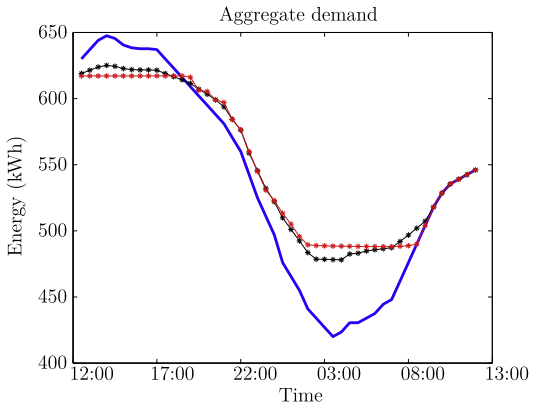

Fig. 5. The non-PEV demand is shown in blue. The aggregate optimal demand is shown in red. The aggregate demand obtained through the V2G HIERARCHICAL algorithm is shown in black.

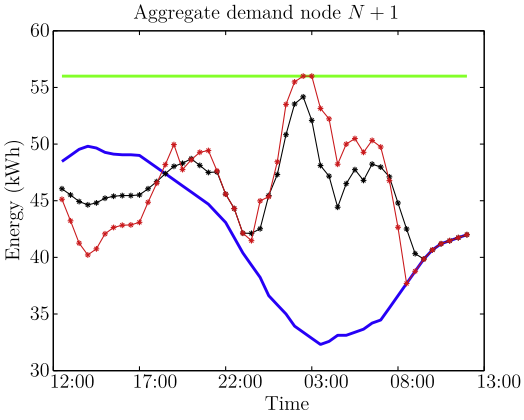

Fig. 6. The non-PEV demand is shown in blue. The optimal aggregate demand is shown in red. The aggregate demand obtained through the V2G HIERARCHICAL algorithm is shown in black. The green line shows the upper bound for the power capacity.

Fig. 6 shows the demand curve for the node $N+1$, with the corresponding transmission line bound (green) for both centralized (red) and hierarchical (black) cases. It can be seen that the solution of the V2G HIERARCHICAL algorithm satisfies the constraint for all time. Fig. 7 shows the same features for the demand at node $N+2$. For our simulation examples, the lower bound on $d_{\ell,\,t}$ is never active. This is mainly due to the ratio between the PEV and non-PEV loads. For node $N+1$, it can be seen that for the optimal solution, there is a t for which $d_{N+1,t} = P^{\max}_{N+1}(t)$.

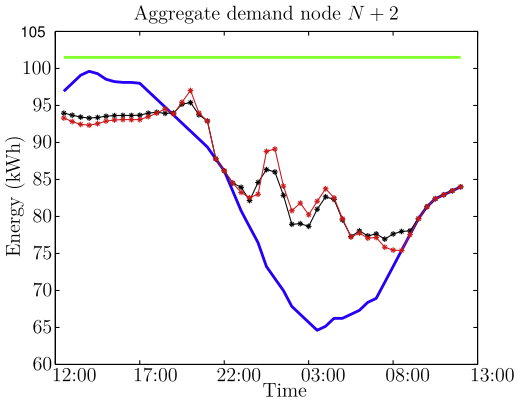

Fig. 7. The non-PEV demand is shown in blue. The optimal aggregate demand is shown in red. The aggregate demand obtained through the V2G HIERARCHICAL algorithm is shown in black. The green line determines upper bound for the power capacity.

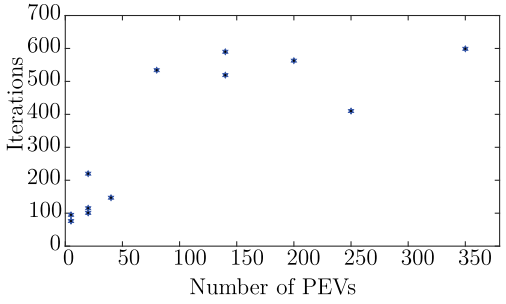

Fig. 8. Dots indicate the number of iterations for which the $\|x_k - x_{k-1}\|^2 < 10^{-8}$.

4.1. Convergence rate

In order to evaluate the impact of the number of PEVs on the V2G HIERARCHICAL algorithm performance, we have generated simulation scenarios with 5, 20, 40, 80, 140, 200, 250, and 350 PEVs respectively. In all cases, battery sizes as well as initial conditions and deadlines have been chosen at random, varying within the same order of magnitude. Two network topologies have been used for this analysis, one corresponds to the one shown in Fig. 3, the other one is a linear graph with seven nodes. For $N = 5,\ 20$ and 140, we have run more than one scenario.

The convergence time is characterized as the number of iterations needed to reach a stopping criterion. Here, the stopping criterion is that the squared length of the step between one iteration and the next is less than 10^{-8}. This metric has been selected based on (18) in the proof of Theorem 3.1, which shows that the function V decreases along the trajectories of the algorithm at a rate proportional to the squared step length.

Fig. 8 shows the convergence time in number of iterations for the different scenarios, versus the number of PEVs in each scenario. It can be seen that there is significant variability in the convergence time between scenarios with the same number of PEVs, probably due to the random characteristics of the problem, which points to the need of further analysis to identify the convergence rate drivers. Nonetheless, the trend appears to indicate that iterations increase with the number of PEVs and that, for the particular scenarios considered, and that the convergence rate is sublinear with respect to the number of PEVs taken.

It is important to mention that for all the simulation scenarios, we solve the optimization problem that does not include the constraint $u_{i,t}v_{i,t} = 0$, for all i, t. However, all obtained solutions

satisfy this constraint, hence they are optimal solutions to the non-relaxed Problem 1.

These simulations have been run using a 2.8 GHz CPU, with 8 GB RAM. A rough study of the simulation time shows that each iteration of the simulation with 80 PEVs takes on average 22.9 seconds, while each iteration of the simulation with 200 PEVs takes on average 47.9 seconds. Notice that we are solving this problem using a single computer, which does not benefit from the parallelization that would occur should the algorithm be implemented in a real scenario. This implies that the quadratic program for each PEV must be taking around 0.28 seconds to be solved. Let us recall that the non-PEV nodes do not have a significant computational burden, since they only have to aggregate loads of their children and communicate the aggregate to their parent nodes.

4.2. Some practical considerations

The implementation of the proposed algorithm requires a particular bundle of communications and processing capacity to carry out the mathematical operations described in Section 3.

On the communications side, the algorithm mostly requires a large amount of transmissions between nodes that are at a relatively short distance within the distribution side of the grid. Moreover, due to the hierarchical structure of the algorithm, it is expected that a single node does not have to exchange information with many others. The largest burden on communications will be due to the potentially high amount of iterations the algorithm may require. However, the volume of communications is also relatively simple, since each node has to transmit at each instant only a vector with T dimensions, and T is not expected to be too large. This means that the communication system can allow a low transmission rate and a relatively low distance between transmitter and receiver. A low cost communication protocol such as Zigbee could be handy for this application on the distribution side. Power-line carrier communication (PLCC), e.g., G3-PLC [26] could also be an alternative to tackle the communication requirement of this algorithm.

The transmission side of the grid requires some information exchange to coordinate the initial energy price to provide the distribution feeders, and this happens at the system level, potentially covering large distances. An ICCP protocol such as the standard IEC 60870-6 which is used to coordinate control center at transmission level could be utilized for this purpose.

On the computation side, computers located at the PEV nodes, either embedded in the PEV or in the charging station must be able to solve the quadratic programs that are required at each iteration of the algorithm. Quadratic programming problems can be solved very efficiently by algorithms that can be executed even with the most inexpensive computation devices, e.g., Arduino, Raspberry-Pi, etc. Additionally, the interface between computation and communications can be easily handled. For instance, most industrial devices, and also computers such as Arduino have available low-cost communication modules for Zigbee protocol.

Due to the convergence times of the proposed algorithms, we believe their applicability is mainly for energy arbitrage or providing energy reserves on a slow time scale. This is an issue that is common to decentralized approaches, where the price of coordination is the convergence time. In addition, possible asynchronous computations may result into suboptimal performance.

On the computation of the parameters η, κ_ℓ for all $\ell \in \mathcal{M}$, the conditions provided by Proposition 2.1, and Theorem 3.1 only depend on parameters of the grid, such as the number of PEVs, and thermal limits on the components of the distribution circuits. Since these parameters are embedded within the coordination signal provided by nodes in $\mathcal{M}$, it means that the calculation can be performed a priori, on the basis of estimates of the operating conditions of the system (e.g., maximum number of PEVs, known thermal limits, etc).

5. Conclusions

We have presented a hierarchical protocol for a vehicle-2-grid (V2G) system in which a fleet of plug-in electric vehicles must coordinate their charging/discharging strategies to minimize a cost function consisting in the price of the total energy provided by the utility during a finite discrete-time horizon. The power flow leaves the transmission side of the power grid and enters the distribution side. The power grid is modeled as a rooted tree, where nodes represent buses in distribution feeders, as well as PEVs. Our model also accounts for power capacity constraints in the distribution lines. In order to account for these constraints, we use penalty functions. In particular, we characterize the size of the constraint violation in terms of the penalty parameters and the parameters of the problem. This characterization provides a design methodology for the choice of the penalization parameters in terms of a desired performance. The presented V2G HIERARCHICAL algorithm does not require communication between PEVs, and the coordination signal is transmitted from the utility down the tree network, while being modified at each non-PEV node, until it reaches the PEVs. Then, each PEV uses it to iterate over its charging/discharging profile. We show that the V2G HIERARCHICAL algorithm converges to the optimizer of the cost function given the network constraints. Simulations show the system behavior for a particular testbed.

Several questions remain open for future work. First, our battery models are linear, simplifying the computation of the optimal solutions of the associated problems. While our algorithm presents a general guideline on how to deal with these models, the consideration of other non-linear or linear parameter-varying system battery models can affect significantly the optimality and computation of the solutions. As a future direction, we also aim to address the power constraints in the elements subject to capacity constraints using non-differentiable penalty functions that allow exact solutions of the original problem, but require a subgradient-based algorithm for the solution, with the ensuing complications in the analysis.

Appendix A. Proof of Lemma 2.1

For the proof of Lemma 2.1, we proceed by contradiction, by showing that if u, v is a feasible solution to the relaxed version of Problem 1, satisfying constraints (5b), (5f), and (5g) strictly and such that (3d) holds as $-P_\ell^{\max}(t) + \epsilon < d_{\ell,t} \leq P_\ell^{\max}(t)$, for $\epsilon \geq u_{\max}(1 - \max_{i\in\mathcal{N}} \alpha_i^c \alpha_i^d)$ then it must also satisfy constraint (5h) in order for it to be optimal.

Assume then that there is a unique pair $i \in \mathcal{N}$ and a $t \in \tau$ such that $u_{i,t} v_{i,t} > 0$ (the case of other nodes and times can be treated independently.) Define a new profile $(\bar{u}, \bar{v})$ such that $\bar{u}_{j,q} = u_{j,q}$ and $\bar{v}_{j,q} = v_{j,q}$ for all $(j,\ q) \neq (i,\ t)$, and $\bar{u}_{i,t} = \gamma \max\{0, u_{i,t} - (\alpha_i^c \alpha_i^d)^{-1} v_{i,t}\}$, $\bar{v}_{i,t} = \gamma \max\{0, -(\alpha_i^c \alpha_i^d) u_{i,t} + v_{i,t}\}$. Observe that this profile satisfies the constraints (5c) and (5d) for all $j \in \mathcal{N}$ and $q \in \tau$ and for all $\gamma \in (0,\ 1)$. In particular, we have $\bar{u}_{i,t} \bar{v}_{i,t} = 0$. Since nothing changes for all $(j,\ q) \neq (i,\ t)$, the constraints (5a) in the associated battery variables, $\bar{z}_{j,q}$, also hold. The following can be proven:

1. First, since $u_{i,t}, v_{i,t} > 0$, and $\alpha_i^c, \alpha_i^d \in (0, 1)$, it is easy to see that:

$$\max\{0, u_{i,t} - (\alpha_i^c \alpha_i^d)^{-1} v_{i,t}\} - \max\{0, v_{i,t} - (\alpha_i^c \alpha_i^d) u_{i,t}\} < u_{i,t} - v_{i,t}. \tag{A.1}$$

Therefore, for a sufficiently large $\gamma \in (a_1,\ 1)$ we have that $\bar{u}_{i,t} - \bar{v}_{i,t} < u_{i,t} - v_{i,t}$.

2. The constraints (5b) hold for all $q < t$ (as they hold for (u, v)) and as well for $q \geq t$. To see the latter, note that

$$\bar{z}_{i,t} = z_{i,t},$$
$$\bar{z}_{i,q} = z_{i,q} + \frac{(\gamma-1)}{\beta_i}(\alpha_i^c u_{i,t} - (\alpha_i^d)^{-1} v_{i,t}), \quad q \geq t.$$

Since the constraints (5b) hold strictly on $z_{i,q}$ by assumption, we have that (5b) hold for $\bar{z}_{i,q}$ for all q if we take $\gamma \in (a_2, 1)$. The bound (5g) can be similarly treated.

3. The bounds on the variables $\bar{d}_{\ell,t}$, for $\ell \in \text{an}(i)$, may change as well due to the change in $(\bar{u}, \bar{v})$. We have that

$$\bar{d}_{\ell,t} = L_{\ell,t} + \sum_{\ell' \in \mathcal{M} \cap \text{des}(\ell)} L_{\ell',t} + \sum_{j \in \text{dN}(\ell) \setminus \{i\}} (u_{j,t} - v_{j,t}) + \begin{cases} \gamma(u_{i,t} - (\alpha_i^c \alpha_i^d)^{-1} v_{i,t}), & \text{if } u_{i,t} - (\alpha_i^c \alpha_i^d)^{-1} v_{i,t} \geq 0, \\ \gamma((\alpha_i^c \alpha_i^d) u_{i,t} - v_{i,t}), & \text{if } (\alpha_i^c \alpha_i^d) u_{i,t} - v_{i,t} \leq 0. \end{cases}$$

We first analyze the lower bound of $\bar{d}_{\ell,t}$. If $u_{i,t} - (\alpha_i^c \alpha_i^d)^{-1} v_{i,t} \geq 0$, then $\gamma(u_{i,t} - (\alpha_i^c \alpha_i^d)^{-1} v_{i,t}) = \gamma(u_{i,t} - v_{i,t} + (1 - (\alpha_i^c \alpha_i^d)^{-1}) v_{i,t}) \geq \gamma(u_{i,t} - v_{i,t}) + \gamma(1 - (\alpha_i^c \alpha_i^d)^{-1}) v_{\max}$. If $u_{i,t} - (\alpha_i^c \alpha_i^d)^{-1} v_{i,t} \leq 0$, then $\gamma((\alpha_i^c \alpha_i^d) u_{i,t} - v_{i,t}) = \gamma((-1 + \alpha_i^c \alpha_i^d) u_{i,t} + u_{i,t} - v_{i,t}) \geq \gamma(u_{i,t} - v_{i,t}) + (-1 + \alpha_i^c \alpha_i^d) u_{\max}$. Therefore, in any case, for $\epsilon \geq \max_{i \in \mathcal{N}} \{(1 - (\alpha_i^c \alpha_i^d)^{-1}) v_{\max}, (-1 + \alpha_i^c \alpha_i^d) u_{\max}\}$ we have that $\bar{d}_{\ell,t} \geq d_{\ell,t} + (\gamma - 1)(u_{i,t} - v_{i,t}) - \gamma\epsilon > -P_\ell^{\max}(t) + \epsilon - \gamma\epsilon \geq -P_\ell^{\max}(t) + \epsilon - \epsilon$ for sufficiently large $\gamma \in (a_3, 1)$. Similarly, for the upper bound, we have that, when $u_{i,t} - (\alpha_i^c \alpha_i^d)^{-1} v_{i,t} \geq 0$, then $\gamma(u_{i,t} - (\alpha_i^c \alpha_i^d)^{-1} v_{i,t}) \leq u_{i,t} - v_{i,t}$ for any $\gamma \in (0, 1)$, and, when $u_{i,t} - (\alpha_i^c \alpha_i^d)^{-1} v_{i,t} \leq 0$, (and in the worst case, $u_{i,t} - v_{i,t} < 0$) for $\gamma \in (a_3, 1)$ sufficiently large we have that $\bar{d}_{\ell,t} < P_\ell^{\max}(t)$.

In all, from all the above cases, it is clear that, by choosing a large enough $\gamma \in (\max\{a_1, a_2, a_3\}, 1)$ we can find a new profile $(\bar{u}, \bar{v})$ that is feasible and such that $\bar{u}_{i,t} - \bar{v}_{i,t} < u_{i,t} - v_{i,t}$ with $\bar{u}_{j,q} - \bar{v}_{j,q} = u_{j,q} - v_{j,q}$ for all other (j, q). This implies that the cost function $J(\bar{u}, \bar{v}) < J(u, v)$, a contradiction with (u, v) being optimal.

In particular, when $\alpha_i^c \alpha_i^d = 1$, then one can repeat the previous arguments by taking the constant $\epsilon = 0$ to conclude that the result holds for any profile which is an optimal solution to the relaxed Problem 1 and an interior feasible point.

Finally, if we directly simplify the lower-bound constraints on $d_{\ell,t}$ and just consider upper bounds $d_{\ell,t} \leq P_\ell^{\max}(t)$, then the relaxation is exact for any choice of parameters. To see this, assume again that there is an $i \in \mathcal{N}$ and $t \in \tau$, such that $u_{i,t} v_{i,t} > 0$, then we can construct a strictly better solution. Define $\hat{u}, \hat{v}$, such that $(\hat{u}_{j,q}, \hat{v}_{j,q}) = (u_{j,q}, v_{j,q})$ for all $(j, q) \neq (i, t)$, and $\hat{u}_{i,t} = \max\{0, u_{i,t} - (\alpha_i^c \alpha_i^d)^{-1} v_{i,t}\}$, and $\hat{v}_{i,t} = \max\{0, v_{i,t} - (\alpha_i^c \alpha_i^d) u_{i,t}\}$. Again, it is not difficult to see that $\hat{u}_{j,q}, \hat{v}_{j,q}$ allow the satisfaction of the constraints (5a) through (5g), for all $j \in \mathcal{N}$ and $q \in \tau$. Moreover, since $u_{i,t}, v_{i,t} > 0$, and $\alpha_i^c, \alpha_i^d \in (0, 1)$, from (A.1), we have that $\hat{u}_{i,t} - \hat{v}_{i,t} < u_{i,t} - v_{i,t}$. Then, $\hat{u}, \hat{v}$ is feasible to the relaxed Problem 1 (with the new constraint $\hat{d}_{\ell,t} \leq P_\ell^{\max}(t)$ for $\ell \in \mathcal{M}$ since $\hat{u}_{i,t} - \hat{v}_{i,t} < u_{i,t} - v_{i,t}$). In addition, it follows that $\sum_{j \in \mathcal{N}} (\hat{u}_{j,t} - \hat{v}_{j,t}) < \sum_{j \in \mathcal{N}} (u_{j,t} - v_{j,t})$, and $\sum_{j \in \mathcal{N}} (\hat{u}_{j,q} - \hat{v}_{j,q}) = \sum_{j \in \mathcal{N}} (u_{j,q} - v_{j,q})$, for all $q \neq t$, $q \in \tau$. Given that the function C is convex and increasing, it follows that $J(\hat{u}, \hat{v}) < J(u, v)$, which contradicts that u, v is optimal.

A1. Proof of Proposition 2.1

First, consider an optimal solution $\hat{u}, \hat{v}$ to Problem 2, and an optimal solution $u^\star, v^\star$ to the relaxed version of Problem 1. Notice that:

$$\sum_{t=1}^{T} \sum_{\ell \in \mathcal{M}} \kappa_\ell \Phi_\ell(d_{\ell,t}^\star) = 0,$$

since $u^\star, v^\star$ satisfies all constraints (3d) and (3e). Then, since $\hat{u}, \hat{v}$ is optimal for Problem 2, we have that:

$$J(\hat{u}, \hat{v}) + \sum_{t=1}^{T} \sum_{\ell \in \mathcal{M}} \kappa_\ell \Phi_\ell(\hat{d}_{\ell,t}) \leq J(u^\star, v^\star). \tag{A.2}$$

This is because the optimal solutions $u^\star, v^\star$ for Problem 1 are feasible for Problem 2, therefore the cost of an optimizer of Problem 2 lower bounds the cost of $u^\star, v^\star$ for Problem 2. Next, define $\lambda_{\ell,t}^\star$, for all $\ell \in \mathcal{M}$, as the optimal Lagrange multipliers associated to the constraints in (3d) and (3e) in the relaxed version of Problem 1, which exist by Assumption 2.2 (Slater's condition). Let us define also the Lagrangian function:

$$\mathcal{L}(u, v, \lambda) \triangleq J(u, v) + \sum_{t=1}^{T} \sum_{\ell \in \mathcal{M}} \lambda_{\ell,t}(d_{\ell,t} - P_\ell^{\max}(t)).$$

By Duality Theory [27] and also Assumption 2.2 (Slater's condition) for the relaxed version of Problem 1, we have:

$$J(u^\star, v^\star) = \mathcal{L}(u^\star, v^\star, \lambda^\star) \leq \mathcal{L}(\hat{u}, \hat{v}, \lambda^\star). \tag{A.3}$$

Now, let us proceed by contradiction, to show that

$$\max\{0, \hat{d}_{\ell,t} - P_\ell^{\max}(t)\} \leq \frac{\max_{\eta,t} \lambda_{\eta,t}^\star}{\min_\iota \kappa_\iota} \sqrt{|\mathcal{M}|T}, \tag{A.4}$$

holds for all $\ell \in \mathcal{M}$ and $t \in \tau$. For the sake of clarity, let us introduce the vector $\mathbf{g}(u, v) \in \mathbb{R}^s$, where $s \triangleq |\mathcal{M}|T$, and with components $\max\{0, d_{\ell,t} - P_\ell^{\max}(t)\}$, for all ℓ, t.

Assume that $\hat{u}, \hat{v}$ is such that $\max\{0, \hat{d}_{\ell,t} - P_\ell^{\max}(t)\} > \sqrt{s}\xi$, where $\xi \triangleq \max_{\eta,t} \lambda_{\eta,t}^\star / \min_\iota \kappa_\iota$, for some $\ell \in \mathcal{M}$, $t \in \tau$. This is equivalent to saying that $\|\mathbf{g}(\hat{u}, \hat{v})\|_\infty > \sqrt{s}\xi$. Since $\sqrt{s}\xi > 0$, we can multiply on both sides by $\|\mathbf{g}(\hat{u}, \hat{v})\|_1$ and move $\sqrt{s}$ to the left-hand side to obtain

$\|\mathbf{g}(\hat{u}, \hat{v})\|_1 \|\mathbf{g}(\hat{u}, \hat{v})\|_\infty / \sqrt{s} > \xi \|\mathbf{g}(\hat{u}, \hat{v})\|_1$. By properties of norms, we have that $\|\mathbf{g}(\hat{u}, \hat{v})\|_2 \geq \|\mathbf{g}(\hat{u}, \hat{v})\|_\infty$, and also $\|\mathbf{g}(\hat{u}, \hat{v})\|_2 \geq \|\mathbf{g}(\hat{u}, \hat{v})\|_1 / \sqrt{s}$. Then, it follows that $\|\mathbf{g}(\hat{u}, \hat{v})\|_2^2 \geq \|\mathbf{g}(\hat{u}, \hat{v})\|_1 \|\mathbf{g}(\hat{u}, \hat{v})\|_\infty / \sqrt{s} > \xi \|\mathbf{g}(\hat{u}, \hat{v})\|_1$, which implies that:

$$\sum_{t=1}^{T} \sum_{\ell \in \mathcal{M}} \Phi(\hat{d}_{\ell,t}) > \sum_{t=1}^{T} \sum_{\ell \in \mathcal{M}} \xi \max\{0, \hat{d}_{\ell,t} - P_\ell^{\max}(t)\} \geq \sum_{t=1}^{T} \sum_{\ell \in \mathcal{M}} \frac{\max_{\eta,t} \lambda_{\eta,t}^\star}{\min_\iota \kappa_\iota} (\hat{d}_{\ell,t} - P_\ell^{\max}(t)).$$

By multiplying both sides of the previous equation by $\min_\iota \kappa_\iota$, it is easy to see that:

$$\sum_{t=1}^{T} \sum_{\ell \in \mathcal{M}} \kappa_\ell \Phi(\hat{d}_{\ell,t}) > \sum_{t=1}^{T} \sum_{\ell \in \mathcal{M}} \lambda_{\ell,t}^\star (\hat{d}_{\ell,t} - P_\ell^{\max}(t)),$$

which in turn implies that:

$$\mathcal{L}(\hat{u}, \hat{v}, \lambda^\star) < J(\hat{u}, \hat{v}) + \sum_{t=1}^{T} \sum_{\ell \in \mathcal{M}} \kappa_\ell \Phi_\ell(\hat{d}_{\ell,t}). \tag{A.5}$$

From Equations (A.2), (A.3), and (A.5), it follows that $J(u^\star, v^\star) < J(u^\star, v^\star)$, a contradiction. Hence, (A.4) must hold for all $\ell \in \mathcal{M}$, $t \in \tau$.

Now, from [28, Chapter 10], we have that:

$$\max_{\ell,t} \lambda_{\ell,t}^\star \leq \frac{1}{\gamma}(J(\bar{u}, \bar{v}) - \bar{J}),$$

where $\bar{J} = J(\tilde{u}, \tilde{v})$, $\tilde{u}, \tilde{v}$ is a solution to the relaxed version of Problem 1, without the constraints (3d) and (3e), $\bar{u}, \bar{v}$ is a Slater vector of Problem 1, and $\gamma \triangleq \min_{\ell,t} P_\ell^{\max}(t) - \bar{d}_{\ell,t}$. Note that by definition of Slater vector, $u^\dagger, v^\dagger$ as described in Assumption 2.2 is a Slater

vector of Problem 1 and that $\epsilon \le \gamma$. Since C is increasing, we have that:

$$\sum_{t=1}^{T} C(-P_{\mathbf{r}}^{\max}(t)) \le J(\bar{u}, \bar{v}) \le \sum_{t=1}^{T} C(P_{\mathbf{r}}^{\max}(t)),$$

from (3e). Thus, defining $J_{\max} = \sum_{t=1}^{T} C(P_{\mathbf{r}}^{\max}(t))$ and $J_{\min} = \sum_{t=1}^{T} C(-P_{\mathbf{r}}^{\max}(t))$, and using that $\gamma \ge \varepsilon$, we have that

$$\max_{\ell,t} \lambda^{\star}_{\ell,t} \le \frac{1}{\varepsilon}(J_{\max} - J_{\min}). \tag{A.6}$$

Now, from (A.4), we have that

$$\hat{d}_{\ell,t} - P_{\ell}^{\max}(t) \le \frac{\max \lambda^{\star}_{\eta,t}}{\min_{\iota} \kappa_{\iota}} \sqrt{T|\mathcal{M}|}.$$

Plugging into the inequality for (A.6) and the definition of κ_{ℓ} of the proposition, we have that

$$\begin{aligned}\hat{d}_{\ell,t} - P_{\ell}^{\max}(t) &\le \frac{(J_{\max} - J_{\min})\sqrt{T|\mathcal{M}|}\sigma \min_{\iota} P_{\iota}^{\max}(t)}{\varepsilon\sqrt{T|\mathcal{M}|}(J_{\max} - J_{\min})} \\ &\le \sigma P_{\ell}^{\max}(t),\end{aligned}$$

from which the result follows.

Appendix B. Optimality characterization [27]

For the feasible convex optimization problem:

minimize: $f(x)$,

subject to:

$x \in X$,

with $x \in \mathbb{R}^n$, $x^{\star}$ is an optimizer if and only if:

$\nabla f(x^{\star})^{\top}(x - x^{\star}) \ge 0$,

for all $x \in X$.

B1. Auxiliary results

Lemma B.1 (Counting of edges in $\mathcal{T}$). *The equality:*

$$\sum_{\ell \in \mathcal{M}\setminus\{\mathbf{r}\}} \sum_{i \in \mathrm{dN}(\ell)} A_i B_{\ell} = \sum_{i \in \mathcal{N}} \sum_{\ell \in \mathrm{an}(i)\setminus\{\mathbf{r}\}} A_i B_{\ell},$$

holds for any terms A_i, B_{ℓ}.

Proof. It is easy to show that each of the summands accounts for one path between each PEV and each of its ancestors. □

References

[1] J.A.P. Lopes, F.J. Soares, P.M.R. Almeida, Integration of electric vehicles in the electric power system, Proceedings of the IEEE 99 (1) (2011) 168–183.

[2] K. Mets, T. Verschueren, W. Haerick, C. Develder, F.D. Turck, Optimizing smart energy control strategies for plug-in hybrid electric vehicle charging, in: IEEE/IFIP Network Operations and Management Symposium (NOMS) Workshops, 2010, pp. 293–299.

[3] A.S. Masoum, S. Deilami, P.S. Moses, M.A.S. Masoum, A. Abu-Siada, Smart load management of plug-in electric vehicles in distribution and residential networks with charging stations for peak shaving and loss minimisation considering voltage regulation, IET Generation, Transmission & Distribution 5 (8) (2011) 877–888.

[4] P. Richardson, D. Flynn, A. Keane, Optimal charging of electric vehicles in low–voltage distribution systems, IEEE Transactions on Power Systems 27 (1) (2012) 268–279.

[5] O. Sundström, C. Binding, Flexible charging optimization for electric vehicles considering distribution grid constraints, IEEE Transactions on Smart Grid 3 (1) (2012) 26–37.

[6] Z. Ma, D.S. Callaway, I.A. Hiskens, Decentralized charging control of large populations of plug-in electric vehicles, IEEE Transactions on Control Systems Technology 21 (1) (2011) 67–78.

[7] L. Gan, U. Topcu, S.H. Low, Optimal decentralized protocol for electric vehicle charging, IEEE Transactions on Power Systems 28 (2) (2013) 940–951.

[8] A. Cortés, S. Martínez, A hierarchical algorithm for optimal plug-in electric vehicle charging with usage constraints, Automatica 68 (2016) 119–131.

[9] Y. He, B. Venkatesh, L. Guan, Optimal scheduling for charging and discharging of electric vehicles, IEEE Transactions on Smart Grid 3 (3) (2012) 1095–1105.

[10] W. Ma, V. Gupta, U. Topcu, On distributed charging control of electric vehicle with power network capacity constraints, in: American Control Conference, 2014, pp. 4306–4311.

[11] Z. Li, Q. Guo, H. Sun, H. Su, ADMM-based decentralized demand response method in electric vehicle virtual power plant, in: IEEE Power and Energy Society General Meeting, 2016, pp. 1–5.

[12] Z. Ma, N. Yang, S. Zou, Y. Shao, Charging coordination of plug-in electric vehicles in distribution networks with capacity constrained feeder lines, IEEE Transactions on Control Systems Technology (2017) 1–8.

[13] S. Zou, I. Hiskens, Z. Ma, Decentralized coordination of controlled loads and transformers in a hierarchical structure, IFAC PapersOnLine 50 (1) (2017) 5560–5566.

[14] J. Rivera, P. Wolfrum, S. Hirche, C. Goebel, H. Jacobsen, Alternating direction method of multipliers for decentralized electric vehicle charging control, in: IEEE Int. Conf. on Decision and Control, IEEE, 2013, pp. 6960–6965.

[15] Z. Ma, S. Zou, X. Liu, A distributed charging coordination for large-scale plug-in electric vehicles considering battery degradation cost, IEEE Transactions on Control Systems Technology 23 (5) (2015) 2044–2052.

[16] T. Sousa, Z. Vale, J.P. Carvalho, T. Pinto, H. Morais, A hybrid simulated annealing approach to handle energy resource management considering an intensive use of electric vehicles, Energy 67 (2014) 81–96.

[17] A.T. Al-Awami, E. Sortomme, Coordinating vehicle-to-grid services with energy trading, IEEE Transactions on Smart Grid 3 (1) (2012) 453–462.

[18] C. Wu, H. Mohsenian-Rad, J. Huang, Vehicle-to-aggregator interaction game, IEEE Transactions on Smart Grid 3 (1) (2012) 434–442.

[19] A. Cortés, S. Martínez, A hierarchical demand-response mechanism for optimal vehicle-to-grid coordination, in: European Control Conference, (Linz, Austria), 2015, pp. 2420–2425. July

[20] J. Manwell, J. McGowan, Lead acid battery storage model for hybrid energy systems, Solar Energy 50 (5) (1993) 399–405.

[21] M. Stadler, C. Marnay, M. Kloess, G. Cardoso, G. Mendes, A. Siddiqui, R. Sharma, O. Mégel, J. Lai, Optimal planning and operation of smart grids with electric vehicle interconnection, Journal of Energy Engineering 138 (2) (2012) 95–108.

[22] D.P. Bertsekas, Necessary and sufficient conditions for a penalty method to be exact, Mathematical Programming 9 (1) (1975) 87–99.

[23] S. Boyd, N. Parikh, E. Chu, B. Peleato, J. Eckstein, Distributed optimization and statistical learning via the alternating direction method of multipliers, Foundations and Trends in Machine Learning 3 (1) (2010) 1–122.

[24] E. Wei, A. Ozdaglar, On the O(1/k) convergence of asynchronous distributed alternating direction method of multipliers, in: Global conference on signal and information processing (GlobalSIP), 2013, IEEE, 2013, pp. 551–554.

[25] A. Nedić, A. Ozdaglar, Subgradient methods for saddle-point problems, Journal of Optimization Theory & Applications 142 (1) (2009) 205–228.

[26] G3-PLC alliance, 2016, March Website http://www.g3-plc.com.

[27] S. Boyd, L. Vandenberghe, Convex Optimization, Cambridge University Press, 2004.

[28] D.P. Palomar, Y.C. Eldar, Convex optimization in signal processing and communications, Cambridge University Press, 2010.